Structure and thermodynamics of Fe_{55}, Co_{55}, and Ni_{55} clusters supported on a surface

U. Sarkar* and S. A. Blundell†
Service de Physique Statistique, Magnétisme et Supraconductivité, INAC, CEA-Grenoble/DSM, 17 rue des Martyrs, F-38054 Grenoble Cedex 9, France
(Received 22 December 2008; published 31 March 2009)

We study the structure and thermodynamics of Fe_{55}, Co_{55}, and Ni_{55} clusters supported on a surface. The metallic bonding is described by a Gupta potential, and the surface is modeled by an idealized smooth plane coupled to the cluster by a Lennard-Jones interaction, with a variable parameter to describe the strength of the cluster-surface interaction. Optimum (lowest-energy) structures are determined by regular quenches, and the caloric curve of the clusters is extracted via a microcanonical multihistogram fit as a function of the cluster-surface interaction strength. The optimum structures are icosahedral for the free clusters and go through a series of transformations as the cluster-surface interaction strengthens, becoming successively flatter. The melting temperatures of the cluster correspondingly go through a series of steps with each change in optimum structure, but with an average trend toward higher melting temperatures as the cluster-surface interaction increases.

DOI: 10.1103/PhysRevB.79.125441 PACS number(s): 65.80.+n, 61.46.Bc, 64.70.D−, 64.70.Nd

I. INTRODUCTION

The physical and chemical properties of small atomic and molecular clusters can be very different from those of the corresponding bulk material.[1] For example, the enhanced ratio of surface to volume for a small system and quantum confinement effects can both play a significant role in modifying bulk properties. The structural and bonding characteristics of clusters can in consequence differ markedly from those of the bulk.[2] Experiments have also shown that the thermodynamic and melting properties of small clusters can have peculiar properties. Sodium clusters in the size range $N=50-200$ atoms have melting temperatures that vary irregularly with respect to the cluster size.[3,4] Also, small clusters of Sn and Ga have been shown to have melting temperatures higher that of the bulk,[5,6] in contrast to the usual paradigm in which a small particle should melt at a lower temperature than the bulk because of the effect of the surface. The explanation for this has been traced to a change in the nature of the bonding between the cluster and the bulk; the former showing a bond of highly covalent character.[7,8] The structural properties of small clusters supported on a surface have also been demonstrated to be modified by the interaction with the surface, both experimentally[9–12] and theoretically.[10,11,13,14]

In the present paper, we consider the effects of a support on the structure and melting temperatures of three transition-metal clusters. Supported transition-metal clusters such as Ni, Co, Fe, and their alloys have important uses for catalyzing the growth of carbon nanotubes (CNTs).[15,16] The size of the clusters, the temperature, and the nature of the cluster-surface interaction, together with other experimental parameters such as the pressure, are important for determining the characteristics of the CNTs, including their diameter and quality. The detailed mechanism of CNT growth is not well understood. For instance, different combinations of cluster and surface materials can produce marked changes in the efficiency of the process and it would be highly desirable to find a way to control the chirality of the nanotubes that are produced. For these reasons, there has been considerable interest recently in the simulation of the cluster-catalyzed CNT growth process.[17–25]

With this motivation, Ding *et al.*[17] and Shibuta and Maruyama[18] recently considered the effect of the cluster-surface interaction on the melting temperatures of supported Fe and Ni clusters, respectively. The clusters they considered contained upwards of 150 Fe atoms[17] or 256 Ni atoms,[18] and the surface was modeled as an idealized smooth plane coupled to the cluster via an effective interaction of Lennard-Jones type. They treated the cluster-surface interaction strength as a variable parameter, finding that the melting temperatures T_m of the clusters increased monotonically as the strength of the cluster-surface interaction increased.

However, single-walled carbon nanotubes are often grown from smaller clusters containing upwards of only several tens of atoms.[15] At these small sizes, the clusters can have distinct structures dominated by geometric effects.[1,2] Therefore, in this paper we study the structure and thermodynamics of these smaller clusters. Our main aim is to consider the possible effects on the cluster thermodynamics of the specific structural changes that occur at these smaller sizes as a function of the cluster-surface interaction strength. We choose clusters of size 55 because it is quite well established that free metallic clusters (at least for classical interatomic potentials) have a complete two-shell Mackay icosahedral structure for this size, conferring upon the clusters a certain degree of geometrical stability.[1] Using a similar model to that of Ding *et al.*[17] and Shibuta and Maruyama[18] for the cluster and cluster-surface interaction, we first extract the optimum (lowest-energy) structures of the cluster by means of a method of regular quenches from high-temperature runs. Next, by slowly heating the clusters from their optimum structure, we extract the classical density of states $\Omega(E)$ for the ionic motion by means of a microcanonical multihistogram fit.[26] We find a series of distinct structural changes as the cluster-surface interaction strength increases, reflected in a detailed pattern of steps in the melting temperatures associated with each structural transformation.

TABLE I. Parameters of the SMA potential assumed for Fe, Co, and Ni clusters.

Atom	A (eV)	ξ (eV)	p	q	r_0 (Å)
Fe[a]	0.13315	1.6179	10.50	2.60	2.553
Co[b]	0.0950	1.4880	11.604	2.286	2.497
Ni[c]	0.0376	1.070	16.999	1.189	2.490

[a]References 31 and 32.
[b]References 30 and 33.
[c]References 30 and 34.

The paper is organized as follows. In Sec. II, we outline our model and simulation methods. Then, in Sec. III, we present the structures and thermodynamic results for the clusters as a function of the cluster-surface interaction strength. The conclusions are given in Sec. IV

II. MODEL AND METHODOLOGY

In this work we use classical molecular dynamics[27] (MD) with the metallic bonding described by a many-body Gupta potential derived within the tight-binding second-moment approximation.[28–30] The total energy of a free cluster in this approach is given by

$$E_{\text{free}} = A\sum_i \sum_{j\neq i} \exp\left[-p\left(\frac{R_{ij}}{r_0}-1\right)\right] - \xi\sum_i \left\{\sum_{j\neq i} \exp\left[-2q\left(\frac{R_{ij}}{r_0}-1\right)\right]\right\}^{1/2}, \quad (1)$$

where R_{ij} is the distance between ions i and j. The parameters that we use for Fe, Co, and Ni have been obtained by fitting bulk cohesive energies, lattice parameters, and elastic constants; they are summarized in Table I with references to the original work where they were derived, as well as to some related works.

Following Ding *et al.*[17] (and the general approach of Shibuta and Maruyama[18]), we model the surface as an idealized smooth plane that interacts with the cluster via a Lennard-Jones 9/3 potential, yielding an interaction energy

$$E_{\text{surf}} = \varepsilon\frac{3\sqrt{3}}{2}\sum_i \left[\left(\frac{\sigma}{Z_i}\right)^9 - \left(\frac{\sigma}{Z_i}\right)^3\right], \quad (2)$$

where Z_i is the coordinate of ion i perpendicular to the surface. The cluster is in this way constrained to lie near the minimum of the Lennard-Jones well, which is roughly a distance σ above the $Z=0$ plane; we fix $\sigma=0.3$ nm. The parameter ε controls the well depth and hence the overall strength of the cluster-surface interaction. As in Refs. 17 and 18, we treat ε as a variable parameter, taken to lie the range $0\leq\varepsilon\leq 0.9$ eV. The total energy of the cluster plus surface is

$$E_{\text{tot}} = E_{\text{free}} + E_{\text{surf}}. \quad (3)$$

The first step of our approach to simulating the melting properties of the clusters is to search for the global minimum-energy structure. We do this separately for each value of the cluster-surface interaction strength ε, which was allowed to vary from 0 to 0.9 eV in steps of 0.05 eV. We first determine crudely the melting temperatures for a given ε by performing short MD runs (of around 30 ps per temperature) and looking for a step in the caloric curve. Then, we choose a temperature slightly above the expected melting temperature, where the cluster is in a diffusive, liquidlike state, and run a constant-temperature MD simulation (with a Nosé-Hoover heat bath[27]) of duration 200 ps. Structures from this simulation are taken at regular 1 ps intervals and quenched to the nearby local minimum. We repeat this whole procedure three times at slightly different temperatures, giving around 600 local optimizations for each ε. The method tends to be more successful when the simulation temperature is only just above the melting temperature. The best (lowest-energy) three structures found for each ε were retained and put together into a large library of candidate structures for the global minima for all ε.

As a final step, each structure in the entire library of candidate structures was then reoptimized for each value of ε. In this way, even if our regular quenches missed the global minimum for a particular value of ε, there would still be the chance that the structure was found at another (possibly nearby) value of ε and would therefore be revealed in this final pass, as indeed happened in several instances. We only miss the global minimum for a given ε if the corresponding structure was not found in any of the quenches for any ε. While we cannot categorically rule out this possibility, we note that we initially performed only 50 quenches per value of ε and later increased this to 200, with additional simulation temperatures, finding no change in the lowest-energy structures obtained.

Next we determine the caloric curve of the cluster for each ε by sampling the classical density of states via a microcanonical multihistogram fit, following the general procedure described in Refs. 26 and 35. Briefly, for each ε, we start from the lowest-energy structure found by the above procedure and slowly heat the cluster. Microcanonical simulations are performed at 40–50 different total energies within a kinetic temperature range of roughly 200–2500 K. About half of these simulations are distributed between 600 and 1250 K in steps of around 30 K, since this is typically where a meltinglike transition occurs. We perform constant-total-energy (microcanonical) simulations of 200 ps duration for each total energy; the final coordinates and velocities, after scaling, are then used as the initial condition for the next-higher-energy run so that in effect we slowly heat the cluster. Following the microcanonical multihistogram procedure,[26] a least-squares fit to the overlapping histograms of the poten-

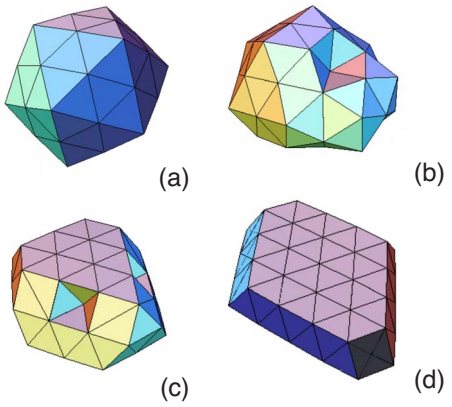

FIG. 1. (Color online) Lowest-energy structures found for Fe_{55} for different values of the cluster-surface interaction strength ε, Eq. (2).

tial energy visited during the simulations allows one to extract the classical density of states $\Omega(E)$ for the ionic motion. This in turn permits the evaluation of thermodynamic averages in a variety of ensembles. For instance, the mean energy (potential plus kinetic) in the canonical ensemble is

$$\langle E\rangle_T = \frac{\int E\Omega(E)e^{-E/kT}dE}{\int \Omega(E)e^{-E/kT}dE}, \tag{4}$$

and an expression for the canonical specific heat may be derived by differentiating this with respect to the temperature T.

III. RESULTS AND DISCUSSION

A. Lowest-energy structures

The lowest-energy structures that we have found for Fe_{55} are shown in Fig. 1 and the variation with ε of the total energy E_{tot} of each of these structures is shown in the upper panel of Fig. 2. We calculated the total energy in this figure by performing a local optimization for each ε, starting with the cluster geometry shown; we checked that the geometry did not change during this optimization. In Fig. 2, we have plotted for each ε the difference between the total energy of a given structure and the total energy of structure (a), so that the relative energies of the various structures are easier to visualize. Within the range of ε considered, there are crossovers among these energy curves, so that each of the structures shown becomes the lowest-energy one for a particular range of ε, as indicated in the figure. Within that range, the structure shown in Fig. 2 had a lower energy than any other structure that we were able to find by our procedure of regular quenches.

The free Fe_{55} cluster ($\varepsilon=0$) is found to be a two-shell Mackay icosahedron, Fig. 1(a). This is in agreement with numerous studies of metallic clusters using the Gupta and Sutton-Chen potentials and is also the case for the Lennard-Jones clusters.[36] For small values of the cluster-surface interaction strength ε, when the cluster-surface interaction is much weaker than the internal interactions within the cluster, the icosahedral geometry remains intact and the cluster orients itself so that one face is parallel to the surface. Eventually, for sufficiently large ε, the icosahedral symmetry breaks and it becomes energetically more favorable to have a slightly elongated, though still quite compact structure [Fig. 1(b)]. As ε increases further, the lowest-energy structure eventually flattens, first into a structure with three ionic layers [Fig. 1(c)] and finally into a two-layer structure [Fig. 1(d)]. The flatter structures lower their energy by increasing the contact area between the cluster and the surface for larger ε.

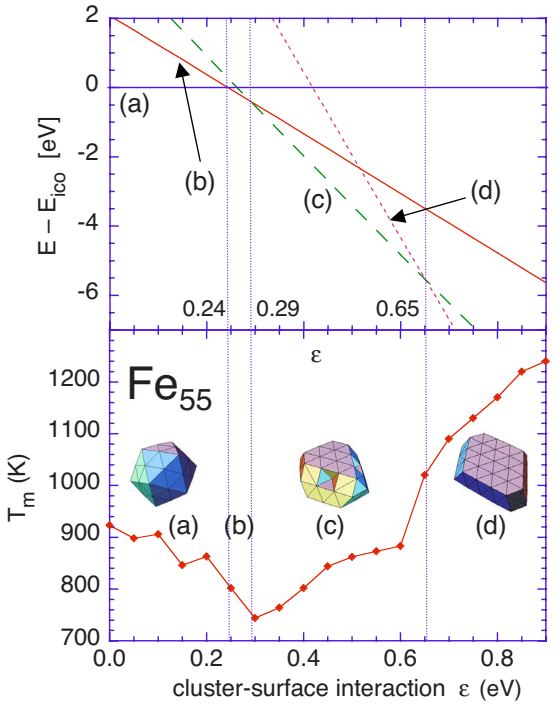

FIG. 2. (Color online) Top panel: Total energy of a Fe_{55} cluster on a surface as a function of the cluster-surface interaction strength ε, Eq. (2), for each of the structures in Figs. 1(a)–1(d). Energies are expressed relative to that of the two-shell Mackay icosahedral structure of Fig. 1(a), which is the lowest-energy structure for $0\leq\varepsilon<0.24$ eV. Structure 1(b) (solid line) is the lowest-energy structure for $0.24\leq\varepsilon<0.29$ eV, structure 1(c) (dashed line) for $0.29\leq\varepsilon<0.65$ eV, and structure 1(d) (short dashed line) for $0.65\leq\varepsilon<0.9$ eV. Bottom panel: Melting temperatures as a function of ε.

For the Co_{55} cluster the situation is qualitatively similar. The structures and energy variation for Co_{55} are shown in Figs. 3 and 4, respectively. After the icosahedral structure breaks, one finds a compact structure [Fig. 3(b)] which is however different from the corresponding Fe_{55} structure [Fig. 1(b)]. This difference is a consequence of the different Gupta parameters assumed for Fe and Co (see Table I). The structure that we found for Fe_{55} is found to be stable also for Co_{55}, but it has a higher energy than the one shown in Fig. 3(b) (by a few tens of meV, depending on the value of ε). For Co_{55} there are two relevant three-layer structures. The first of these [Fig. 3(c)] is quite close to the three-layer structure found for Fe_{55} [Fig. 1(c)]. A rather different three-layer ge-

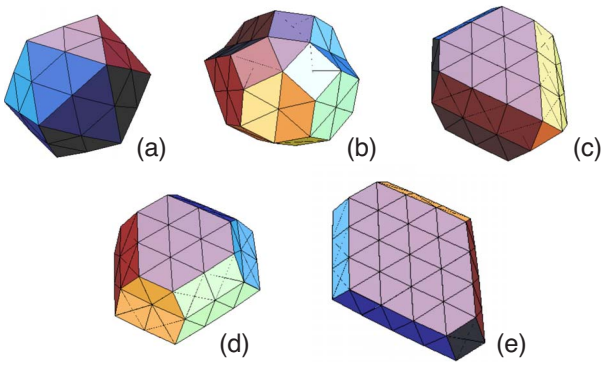

FIG. 3. (Color online) Lowest-energy structures found for Co_{55} for different values of the cluster-surface interaction strength ε, Eq. (2).

ometry [Fig. 3(d)] becomes more stable for larger ε, while for larger ε still one finds the same diamond-shaped two-layer structure [Fig. 3(e)] that occurred for Fe_{55}.

The structures and energy variation for Ni_{55} are shown in Fig. 5 and 6, respectively. The situation is slightly more complex for Ni_{55}. A close inspection of the upper panel of Fig. 6 reveals that, in the range of ε considered, there are six lowest-energy structures (according to our global optimization procedure), which are shown in Figs. 5(a)–5(f). We note from this figure that there is a richer variety of compact structures than for Fe and Co and that Ni_{55} clusters are more robust against flattening, forming only a three-layer structure at the highest ε considered.

We have so far presented only the lowest-energy structures as a function of ε, but the regular quenches revealed

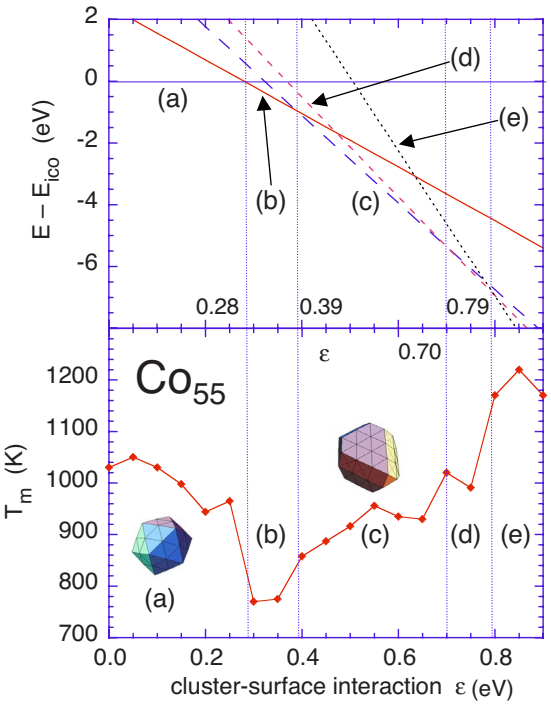

FIG. 4. (Color online) Top panel: Total energy of a Co_{55} cluster on a surface as a function of the cluster-surface interaction strength ε, Eq. (2), for each of the structures in Figs. 3(a)–3(e). Energies are expressed relative to that of the two-shell Mackay icosahedral structure of Fig. 3(a), which is the lowest-energy structure for $0 \leq \varepsilon < 0.28$ eV. Structure 3(b) (solid line) is the lowest-energy structure for $0.28 \leq \varepsilon < 0.39$ eV, structure 3(c) (dashed line) for $0.39 \leq \varepsilon < 0.70$ eV, structure 3(d) (short dashed line) for $0.70 \leq \varepsilon < 0.79$ eV, and structure 3(e) (dotted line) for $0.79 \leq \varepsilon < 0.9$ eV. Bottom panel: Melting temperatures as a function of ε.

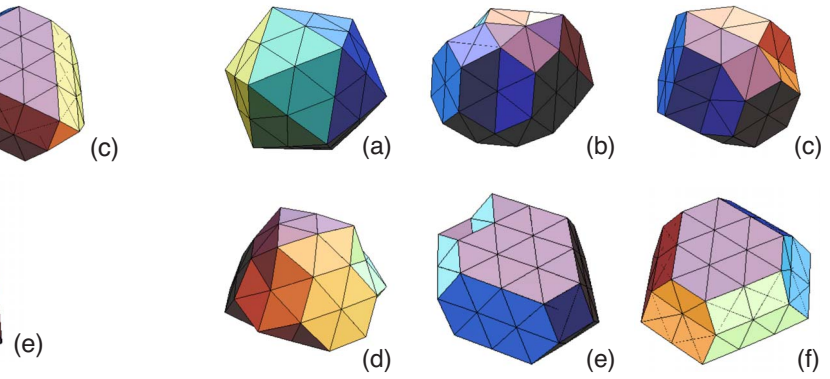

FIG. 5. (Color online) Lowest-energy structures found for Ni_{55} for different values of the cluster-surface interaction strength ε, Eq. (2).

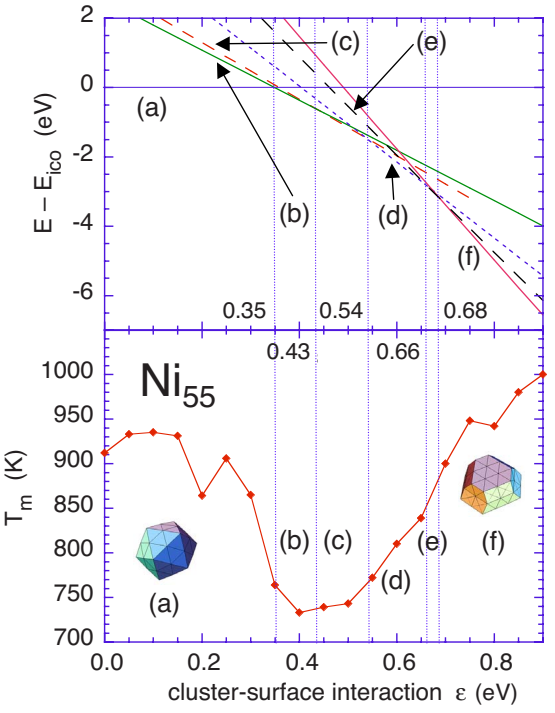

FIG. 6. (Color online) Top panel: Total energy of a Ni_{55} cluster on a surface as a function of the cluster-surface interaction strength ε, Eq. (2), for each of the structures in Figs. 5(a)–5(f). Energies are expressed relative to that of the two-shell Mackay icosahedral structure of Fig. 5(a), which is the lowest-energy structure for $0 \leq \varepsilon < 0.35$ eV. Structure 5(b) (solid line) is the lowest-energy structure for $0.35 \leq \varepsilon < 0.43$ eV, structure 5(c) (dashed line) for $0.43 \leq \varepsilon < 0.54$ eV, structure 5(d) (short dashed line) for $0.54 \leq \varepsilon < 0.66$ eV, structure 5(e) (dashed line) for $0.66 \leq \varepsilon < 0.68$ eV, and structure 5(f) (solid line) for $0.68 \leq \varepsilon < 0.9$ eV. Bottom panel: Melting temperatures as a function of ε.

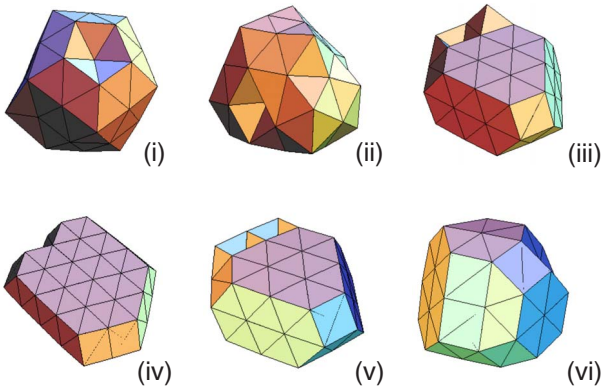

FIG. 7. (Color online) Examples of some excited structures found during the regular quenches. Structures (i)–(v) were found for Fe_{55} and structure (vi) for Co_{55}.

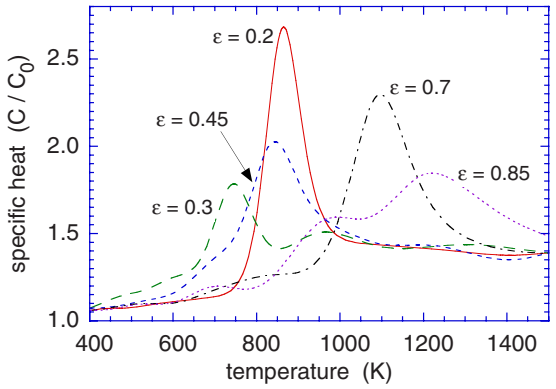

FIG. 8. (Color online) Canonical specific-heat curves of Fe_{55} for various values of the cluster-surface interaction strength ε, Eq. (2), in eV. The specific heat is given as a multiple of the zero-temperature classical limit C_0.

many excited structures as well, some examples of which are shown in Fig. 7. A commonly occurring excited state of the icosahedral structure has one atom from a vertex of the icosahedron (the least tightly bound of the surface atoms) positioned instead above one of the faces, as shown in Fig. 7(i). In general, there are many excited structures that can be regarded as an asymmetric distortion of a lowest-energy structure. For instance, Figs. 7(ii), 7(iii), and 7(iv) are asymmetric distortions of Figs. 1(b)–1(d), respectively. Interestingly, in all the cases we have observed, the lowest-energy structure was found to be one with a high degree of symmetry—thus those in Figs. 1(b)–1(d) rather than Figs. 7(ii), 7(iii), and 7(iv). However, there are also excited structures that are highly symmetric, such as those shown in Figs. 7(v) and 7(vi). All the structures shown have typical excitation energies of order tens of meV or less.

The differences among the observed lowest-energy structures for Fe, Co, and Ni clusters may be attributed, in a complex way, to the differing Gupta parameters in Table I. Now, the Gupta parameters that we have assumed have been obtained by fitting to bulk properties rather than those of finite-sized clusters and these properties also include some bulk elastic constants. However, in the cluster structures we have found, the coordination between a given atom and its neighbors is in general rather different from that found in the bulk periodic lattice. There may also be other finite-size effects related to the surface energy or even to quantum effects (such as shell effects) in the metallic bonding. Since there are evidently many possible structures, with closely spaced energies, it is reasonable to say that the specific lowest-energy structures we have found should be regarded as indicative only. If the assumed interatomic potential is refined slightly, it is possible that some of the lowest-energy structures may change.

As a particular example, we note that the flat structures for Fe_{55} in Figs. 1(c) and 1(d) appear to have fcc(111) layers, while in the bulk the stable low-temperature form of Fe is bcc. In fact, our SMA parameters for Fe (see Table I) have been fitted to properties of bulk γ-Fe (fcc).[31] The SMA potential is well known to be unreliable for bcc structures[30] (which, even if stable at zero temperature, are generally unstable with respect to transformation into fcc at any finite temperature and pressure within the SMA parametrization[30]). It is therefore indeed possible that the packing of atoms in Figs. 1(c) and 1(d) will change if the potential is refined. One way of investigating this possibility might be to use an embedded-atom potential of the type proposed for Fe in Ref. 37, in which the bcc structure is stable; another, more time-consuming approach would be to use first-principles density-functional molecular dynamics.

There exist recent scanning tunneling microscope (STM) images of Fe clusters,[38,39] Co clusters,[40,41] and Ni clusters[42,43] in a size range including $N=55$ atoms on a variety of substrates, but to our knowledge there are no STM images with which we can critically compare our structures in Figs. 1, 3, and 5.

B. Thermodynamics

A sample of specific-heat curves for the clusters is shown in Fig. 8 and two caloric curves are shown in Fig. 9. In most cases, the specific-heat curve has a single dominant peak with a width of about 100–200 K, although in some cases

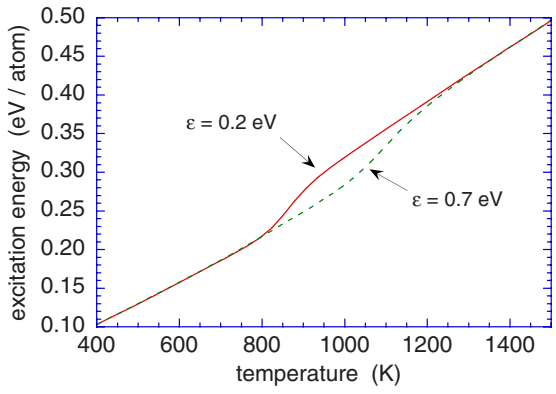

FIG. 9. (Color online) Canonical caloric curves of Fe_{55} for two values of the cluster-surface interaction strength ε, Eq. (2): ε =0.2 eV (solid line) and ε=0.7 eV (dashed line). The quantity plotted on the ordinate is the mean total excitation energy (kinetic energy plus potential energy minus global-minimum potential energy) in the canonical ensemble.

there are also side features. For example, the curve for $\varepsilon = 0.3$ eV in Fig. 8 shows a small side peak at higher temperatures, while that for $\varepsilon = 0.85$ eV has a shoulder on the low-temperature side of the main peak. Inspection of the ionic trajectories suggests that the main peak in these examples corresponds to a "meltinglike" transition.[44] That is, at low temperatures, the ions in the cluster vibrate about fixed points (together with an overall rotation of the cluster), while on the high-temperature side of the peak the cluster is in a diffusive state in which each ion can diffuse throughout the entire volume of the cluster. The meltinglike process is not a sharp phase transition because of the finite number of degrees of freedom of the cluster, and the peak in the specific-heat curve is broadened; one can identify the area under the peak with an approximate latent heat for the process. The side features correspond to additional transformation processes, such as surface rearrangements at low temperatures, and are rather typical for smaller clusters with up to 20 atoms.[44] For the purposes of subsequent discussion, we shall define the "melting temperature" T_m of the cluster as the highest point on the dominant peak of the specific-heat curve.

The melting temperatures T_m for the clusters are shown at intervals of $\Delta\varepsilon = 0.05$ eV in the lower panels of Figs. 2, 4, and 6. For the icosahedral structures at small ε, the T_m are to a first approximation roughly independent of ε to within the expected statistical error on T_m, which we estimate to be of order 5%. However, there is for each cluster an abrupt drop in T_m by 100–200 K when the icosahedral geometry breaks. This is indicative of the particular thermal stability associated with a closed-shell Mackay icosahedron, which has been noted before for free Lennard-Jones[45] and sodium[35] clusters with respect to variations in the cluster size around the "magic" numbers of atoms corresponding to a complete Mackay icosahedron. There also appears to be a trend in which the melting temperature T_m of the icosahedral structure decreases slightly as ε increases even *before* the icosahedral structure finally breaks. This trend is particularly noticeable in the data for Co_{55} [Fig. 4] for ε in the range 0.05–0.2 eV. The slight decrease in melting temperature is presumably indicative of a weakening of the icosahedral structure as it distorts slightly in the presence of the external field due to the surface.

As ε increases further, the variation of T_m is not monotonic, as found for the larger clusters of size several hundred by Ding *et al.*[17] and Shibuta and Maruyama.[18] Instead, in most cases there are distinct steps in the melting temperature whenever the lowest-energy structure changes. The steps are most apparent in the plots for Co in the lower panel of Fig. 4, where the change in T_m across a step can be of order 100 K. The steps reflect the differences in thermal stability that result from the distinct changes in geometry we observe.

Aside from the initial drop in T_m when the icosahedral structure breaks, most of these steps are toward a higher T_m at larger ε, as the lowest-energy structure becomes flatter. There is also, in many cases, a general trend toward higher T_m as ε increases for a given structure. In these respects, the results are analogous to those of Ding *et al.*[17] and Shibuta and Maruyama[18] for larger clusters of size in several hundreds, who found that T_m *increased* monotonically as ε increased.

IV. CONCLUSIONS

Using a simple nonatomistic model of a surface also employed in earlier work,[17,18] we have investigated the structural and melting properties of supported Fe_{55}, Co_{55}, and Ni_{55} clusters. For these small clusters, one finds a rich variety of distinct lowest-energy structures as a function of the cluster-surface interaction strength. The two-shell icosahedral geometry of the free cluster breaks for a sufficiently strong cluster-surface interaction, and the optimum geometry becomes increasingly flatter as the cluster-surface interaction strength increases further. This pattern of structural changes is reflected in a detailed way in the melting temperature of the cluster, which undergoes stepwise changes. Nevertheless, there is an average trend toward higher T_m as the cluster-surface interaction increases, in general agreement with earlier studies[17,18] on clusters of size in several hundreds.

While displaying qualitatively similar behavior, the clusters of Fe, Co, and Ni showed differences in the detailed structures and melting temperatures that, within our model, may only be attributed to the different Gupta parameters assumed. The complexity of the problem and this sensitivity to the parameters suggests that the precise details of the structures we have found may not hold in practice in all cases. A possible way to improve upon the present work would be to use a density-functional-based molecular-dynamics method,[46] which can take account in an *ab initio* way of the size-dependent effects that can be important at these small sizes. While density-functional approaches are orders of magnitude more expensive than the classical MD used here, it has still proved possible to extract caloric curves for free clusters with reasonable statistics.[7] Explicit consideration of the atomistic nature of the surface is likely to modify the detailed structural and thermodynamic properties further.

Nevertheless, the present work gives an indication of the richness of the structures and melting behaviors that are likely to result for these small transition-metal clusters supported on a surface.

ACKNOWLEDGMENTS

We gratefully acknowledge support from the Indo-French Center for the Promotion of Advanced Research (IFCPAR)/Centre Franco-Indien pour la Promotion de la Recherche Avancée (CEFIPRA) under Contract No. 3104-2.

*Present address: LMPGM, Bâtiment C6, University of Science and Technology of Lille, 59655 Villeneuve d'Ascq Cedex, France; utpalchemiitkgp@yahoo.com
†steven.blundell@cea.fr

[1] *Clusters of Atoms and Molecules*, edited by H. Haberland (Springer-Verlag, Berlin, 1995).
[2] *Physics and Chemistry of Finite Systems: From Clusters to Crystals*, edited by P. Jena, S. N. Khanna, and B. K. Rao (Springer-Verlag, Berlin, 1995).
[3] M. Schmidt, R. Kusche, W. Kronmüller, B. von Issendorff, and H. Haberland, Phys. Rev. Lett. **79**, 99 (1997).
[4] M. Schmidt, R. Kusche, B. von Issendorff, and H. Haberland, Nature (London) **393**, 238 (1998).
[5] A. A. Shvartsburg and M. F. Jarrold, Phys. Rev. Lett. **85**, 2530 (2000).
[6] G. A. Breaux, R. C. Benirschke, T. Sugai, B. S. Kinnear, and M. F. Jarrold, Phys. Rev. Lett. **91**, 215508 (2003).
[7] S. Chacko, K. Joshi, D. G. Kanhere, and S. A. Blundell, Phys. Rev. Lett. **92**, 135506 (2004).
[8] K. Joshi, D. G. Kanhere, and S. A. Blundell, Phys. Rev. B **66**, 155329 (2002).
[9] P. R. Schwoebel and G. L. Kellogg, Phys. Rev. Lett. **61**, 578 (1988).
[10] P. R. Schwoebel, S. M. Foiles, C. L. Bisson, and G. L. Kellogg, Phys. Rev. B **40**, 10639 (1989).
[11] H. V. Roy, P. Fayet, F. Patthey, W. D. Schneider, B. Delley, and C. Massobrio, Phys. Rev. B **49**, 5611 (1994).
[12] S. C. Wang and G. Ehrlich, Surf. Sci. **391**, 89 (1997).
[13] A. F. Wright, M. S. Daw, and C. Y. Fong, Phys. Rev. B **42**, 9409 (1990).
[14] J. Zhuang, T. Kojima, W. Zhang, L. Liu, L. Zhao, and Y. Li, Phys. Rev. B **65**, 045411 (2002).
[15] M. S. Dresselhaus, G. Dresselhaus, and P. Avouris, *Carbon Nanotubes: Synthesis, Structure, Properties and Application* (Springer, New York, 2001).
[16] A. A. Puretzky, D. B. Geohegan, X. Fan, and S. J. Pennycook, Appl. Phys. A: Mater. Sci. Process. **70**, 153 (2000).
[17] F. Ding, A. Rosen, S. Curtarolo, and K. Bolton, Appl. Phys. Lett. **88**, 133110 (2006).
[18] Y. Shibuta and S. Maruyama, Chem. Phys. Lett. **437**, 218 (2007).
[19] F. Ding, K. Bolton, and A. Rosen, J. Phys. Chem. B **108**, 17369 (2004).
[20] F. Ding, A. Rosen, and K. Bolton, Phys. Rev. B **70**, 075416 (2004).
[21] F. Ding, A. Rosen, and K. Bolton, J. Chem. Phys. **121**, 2775 (2004).
[22] O. A. Louchev, H. Kanda, A. Rosen, and B. Kim, J. Chem. Phys. **121**, 446 (2004).
[23] S. Maruyama, Y. Murakami, Y. Shibuta, Y. Miyauchi, and S. Chiashi, J. Nanosci. Nanotechnol. **4**, 360 (2004).
[24] K. Bolton, F. Ding, and A. Rosen, J. Nanosci. Nanotechnol. **6**, 1211 (2006).
[25] A. R. Harutyunyan, E. Mora, T. Tokune, B. Kim, A. Rosen, J. Aiqin, N. Awasthi, and S. Curtarolo, Appl. Phys. Lett. **90**, 163120 (2007).
[26] F. Calvo and P. Labastie, Chem. Phys. Lett. **247**, 395 (1995).
[27] J. K. Allen and W. Tildesley, *Computer Simulation of Liquids* (Oxford University Press, Oxford, 1989).
[28] R. P. Gupta, Phys. Rev. B **23**, 6265 (1981).
[29] V. Rosato, M. Guillope, and B. Legrand, Philos. Mag. A **59**, 321 (1989).
[30] F. Cleri and V. Rosato, Phys. Rev. B **48**, 22 (1993).
[31] M. Guillope and B. Legrand, Surf. Sci. **215**, 577 (1989).
[32] J. Stanek, G. Marest, H. Jaffrezic, and H. Binczycka, Phys. Rev. B **52**, 8414 (1995).
[33] L. Zhan, J. Z. Y. Chen, W.-K. Liu, and S. K. Lai, J. Chem. Phys. **122**, 244707 (2005).
[34] G. Moroyoqui-Estrella, E. Urrutia-Bañuelos, and R. Garibay-Alonso, Physica A **374**, 179 (2007).
[35] P. Blaise and S. A. Blundell, Phys. Rev. B **63**, 235409 (2001).
[36] D. J. Wales, J. P. K. Doye, A. Dullweber, M. P. Hodges, F. Y. Naumkin, F. Calvo, J. Hernández-Rojas, and T. F. Middleton, www.wales.ch.cam.ac.uk/CCD.html
[37] H. Chamati, N. I. Papanicolaou, Y. Mishin, and D. A. Papaconstantopoulos, Surf. Sci. **600**, 1793 (2006).
[38] P. N. First, J. A. Stroscio, R. A. Dragoset, D. T. Pierce, and R. J. Celotta, Phys. Rev. Lett. **63**, 1416 (1989).
[39] C. Binns, S. H. Baker, C. Demangeat, and J. C. Parlebas, Surf. Sci. Rep. **34**, 107 (1999).
[40] I. Chado, C. Goyhenex, H. Bulou, and J.-P. Bucher, Phys. Rev. B **69**, 085413 (2004).
[41] H. Bulou and J.-P. Bucher, Phys. Rev. Lett. **96**, 076102 (2006).
[42] Q. Wu and T. E. Madey, Surf. Sci. **555**, 167 (2004).
[43] M. Caffio, A. Atrei, U. Bardi, and G. Rovida, Surf. Sci. **588**, 135 (2005).
[44] R. S. Berry, in *Clusters of Atoms and Molecules*, edited by H. Haberland (Springer-Verlag, Berlin, 1995), Vol. 1.
[45] D. J. Wales and R. S. Berry, J. Chem. Phys. **92**, 4473 (1990).
[46] J. S. Tse, Annu. Rev. Phys. Chem. **53**, 249 (2002).